

## Speed-Adaptive Path-Following Control of a Riderless Bicycle via Road Preview

C.K. Chen<sup>\*</sup>, T.K. Dao<sup>\*\*</sup>

<sup>\*</sup> Professor

Dept. of Mechanical and Automation Engr.

Dayeh University

168 University Rd., Dacun, Changhua, Taiwan

e-mail: ckchen@mail.dyu.edu.tw

<sup>\*\*</sup> Graduate Student

Dept. of Mechanical and Automation Engr.

Dayeh University

### ABSTRACT

In this study, a genetic-fuzzy control system is used to control a riderless bicycle where control parameters can adapt to the speed change of the bicycle. The equations of motion of a bicycle with constraints of rolling-without-slipping contact condition between wheels and ground are developed. This controller consists of two loops: the inner is a roll-angle-tracking controller which generates steering torque, and the outer is a path-following controller which generates the reference roll angle for the inner loop. The inner loop is controlled by a sliding-mode controller (SMC) on the basis of a linear model obtained from the non-linear one via system identification. By defining a stable sliding surface of error dynamics and an appropriate Lyapunov function, the bicycle can reach the roll-angle reference in a finite time and follow that reference without chattering. The outer loop determines the proper reference roll-angle by using a fuzzy-logic controller (FLC) on the basis of preview distance and direction errors. The robustness of the proposed controller against speed change and external disturbances is verified by simulations.

**Keywords:** path following, bicycle control, bicycle dynamics, system identification.

### 1 INTRODUCTION

Since bicycle dynamics is a classical topic in mechanics, much research has been devoted to methods for controlling bicycles. To understand the nature of the dynamics and steering mechanisms of bicycles, Jones [1] conducted a number of investigations. He pointed out that, to balance a manned bicycle, a sufficient centrifugal force can be generated to correct its fall by steering the fork into the direction of the fall. This theory was well formalised mathematically by Bouasse [2], later replicated by Timoshenko and Young [3] and is repeatedly confirmed in common bicycle-riding experience.

Schwab, Meijaard et al. [4][5] developed linearised equations of motion for a bicycle as a benchmark. In their study, the numerical multibody dynamics program SPACAR and the symbolic software AutoSim®, were compared for validation. Extended equations were later given by Meijaard and Schwab [6], and also further discussed by Sharp [7], including acceleration effects, finite cross-section tires, tire forces and dynamics, as well as both frame and rider compliances.

As an unstable and underactuated system, the bicycle is control-challenging; thus, it can offer a number of research possibilities in the area of mechanics and robot control. Control efforts for stabilising unmanned bicycles have also been addressed in previous studies. Yavin [8] dealt with the stabilisation and control of an unmanned bicycle by both a pedalling and a directional torque, as well as a rotor mounted on the crossbar that generated a tilting torque. Beznos et al.

[9] modelled a bicycle with gyroscopes that enabled the vehicle to stabilise itself in autonomous motions along both a straight line and a curve. In their study, the stabilisation unit consisted of two coupled gyroscopes spinning in opposite directions. Han et al. [10] derived a simple kinematic and dynamic formulation of an unmanned electric bicycle. The controllability of the stabilisation problem was also verified and a control algorithm for self-stabilisation of the vehicle with a bounded wheel speed and steering angle, by using a nonlinear control based on a sliding patch and stuck phenomena, was proposed.

Getz [11] applied internal equilibrium control to the problem of path-following with balance for a bicycle. From the internal dynamics of the bicycle, an internal equilibrium manifold, a sub-manifold of the state-space, was constructed. Among studies pertaining to two-wheeled-vehicle control, Sharp et al. [12] presented a related work on the roll-angle-tracking of motorcycles. A PID controller was used to generate the steering torque on the basis of the tracking error. The PID gains were variant related to the speed of the motorcycle, making the controller adaptive to the speed change. In other studies, Sharp applied an optimal linear preview control theory to the steering control of a bicycle [7] via the benchmark model developed in [4] and [5] with extensions discussed in the same paper. The same theory was applied to a motorcycle [13] via a linear model generated by AutoSim®.

In previous studies of Chen et al. [14][15][16], a diversity of works has been introduced relative to the dynamics and control of an unmanned bicycle. When changing the direction of a bicycle, the rider must always control the roll angle. This implies that the roll-angle control is a preliminary step for developing the turning or path-tracking controllers [15]. The roll-angle-tracking control structures presented in [14] and [16], which are based on fuzzy-logic controllers (FLCs), demonstrated that the bicycle could follow the roll-angle command with only a small tracking error. However, these control structures are model-free and the fuzzy control parameters are sensitive to speed change. The control parameters tuned for a certain speed may not be used to properly control the bicycle at another speed.

In this study, a control structure using sliding mode control (SMC) is designed to address this problem. With the information of the system model, this controller design would be more accurate and robust to the effects of parameter variation and disturbance. First, an approach using system identification techniques is applied to determine a linear model from the input-output data of the nonlinear bicycle model at a specific speed. The bicycle dynamic model described in a previous study [14] is used with configuration parameters adopted from the benchmark bicycle [5]. The input steering torque signal and output data, including roll and steering angles, are generated from a roll-angle control simulation via a simple PD controller; however, the control performance is not an issue in this phase. In this way, a speed-specific linear model can be obtained. From the linear model, a roll-angle controller is designed by using sliding mode control. The control simulations demonstrated that the controller can control the bicycle with a small tracking error and robustness against speed variations, as well as external disturbances.

The remainder of this paper is organised as follows. In Section 2, the nonlinear bicycle model is briefly reviewed. In Section 3, the system identification method, the sliding-mode control process for the roll-angle tracking, and the path-tracking controller with preview and disturbance rejection are explained. The identified results for different speeds and control results are presented and discussed in Section 4. Finally, concluding remarks are given in Section 5.

## 2 BICYCLE MODEL

### 2.1 Nonlinear model

In this study, the bicycle model with nine generalised coordinates and two algebraic variables, presented in [14] and [15] (Figure 1), is used. The dynamics of the bicycle are described by the motion of a reference point  $c$ . Six coordinates are used to designate the positions and orientations of the body at point  $c$ . The other three coordinate variables are the steering angle  $\delta$ , and the rotating angles  $\phi_r$  and  $\phi_f$  of the rear and front wheels. According to the foregoing definitions, the generalised coordinates  $\mathbf{q}$  can be written as



point and longitudinal speed  $v$  is so small that  $\dot{y}/v$  can be approximated by the yaw angle  $\psi$ . By these assumptions, the original nonlinear model can be linearised as

$$\mathbf{M}\ddot{\mathbf{q}} + v\mathbf{C}_1\dot{\mathbf{q}} + (g\mathbf{K}_0 + v^2\mathbf{K}_2)\mathbf{q} = \mathbf{f}, \quad (3)$$

where  $\mathbf{q} = [\theta, \delta]^T$  is the vector composed of the roll and steering angles, respectively;  $\mathbf{f} = [0, \tau]^T$ , the force vector consisting of the steering torque  $\tau$ ;  $v$ , the bicycle forward speed;  $g$ , the gravity; and  $\mathbf{M}$ ,  $\mathbf{C}_1$ ,  $\mathbf{K}_0$  and  $\mathbf{K}_2$ , the bicycle-dependant constant coefficient matrices. Due to the aforementioned assumptions and the system order reduction on which this linearisation approach is based, certain dynamic properties may be lost. Furthermore, although parameters  $\mathbf{M}$ ,  $\mathbf{C}_1$ ,  $\mathbf{K}_0$  and  $\mathbf{K}_2$  are constant coefficient matrices, they are dependent on the physical characteristics of the bicycle and, hence, not so straightforward to measure. This dependence can be a source of uncertainties in the mathematical model as well. For these reasons, system identification is applied in this study to determine the parameters of the linear model at a specific speed.

### 3 CONTROL DESIGN

#### 3.1 System-identification approach

The identification of a dynamic system is achieved by the extraction of its mathematical model from the input and output measurements. System identification is a broad topic which appears in almost all areas of control and modelling theory. Many identification methods have been proposed on the basis of the characteristics of the models to be estimated, such as linear or nonlinear, time or frequency domain, and parametric or nonparametric. In this study, a prediction-error method [18] is used to identify the bicycle state-space model in canonical form.

First, equation (3) can be rewritten as

$$\ddot{\mathbf{q}} = -\mathbf{M}^{-1} [v\mathbf{C}_1\dot{\mathbf{q}} + (g\mathbf{K}_0 + v^2\mathbf{K}_2)\mathbf{q}] + \mathbf{M}^{-1}\mathbf{f}. \quad (4)$$

By choosing the state vector as

$$\mathbf{x} = [\theta, \dot{\theta}, \delta, \dot{\delta}]^T, \quad (5)$$

the state-space model can be expressed in canonical form as

$$\begin{aligned} \dot{\mathbf{x}} &= \mathbf{A}\mathbf{x} + \mathbf{B}\tau, \\ \mathbf{y} &= \mathbf{C}\mathbf{x}, \end{aligned} \quad (6)$$

where  $\mathbf{A} = \begin{bmatrix} 0 & 1 & 0 & 0 \\ a_1 & a_2 & a_3 & a_4 \\ 0 & 0 & 0 & 1 \\ a_5 & a_6 & a_7 & a_8 \end{bmatrix}$ ,  $\mathbf{B} = \begin{bmatrix} 0 \\ b_1 \\ 0 \\ b_2 \end{bmatrix}$  and  $\mathbf{C} = \begin{bmatrix} 1 & 0 & 0 & 0 \\ 0 & 0 & 1 & 0 \end{bmatrix}$ . It can be derived from (4)

and (6) that

$$a_i = \begin{cases} \alpha_i + \beta_i v^2, & i = 1, 3, 5, 7, \\ \alpha_i v, & i = 2, 4, 6, 8, \end{cases} \quad (7)$$

where  $\alpha_i$  and  $\beta_i$  are constants dependent on  $\mathbf{M}$ ,  $\mathbf{C}_1$ ,  $\mathbf{K}_0$  and  $\mathbf{K}_2$ ; and  $b_{i=1,2}$  are constants dependent on  $\mathbf{M}$ . From equation (7), a bicycle running at a constant speed can be modeled as equation (6), with constant matrices  $\mathbf{A}$  and  $\mathbf{B}$ . Therefore, in the following system identification process, model (6) is used since the bicycle is identified at a constant speed.

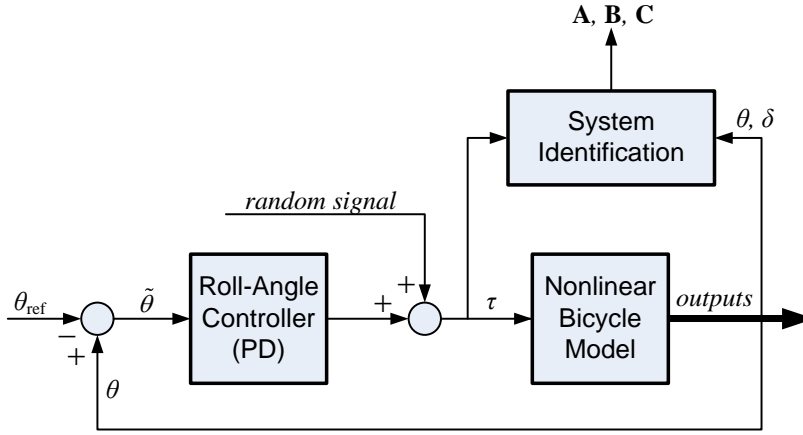


**Figure 2.** System-identification schematic.

Canonical parameterisation represents a state-space system in its minimal form; that is, the system dynamics are expressed by using a minimal number of free parameters. In system (6), the free parameters  $\boldsymbol{\theta} = [a_{i=1..8} \quad b_{i=1,2}]^T$  appear in only the second and fourth rows in the system matrices  $\mathbf{A}$  and  $\mathbf{B}$ , and the remaining matrix elements are fixed to either zeros or ones. By this parameterisation, the numerical Gauss-Newton method can be used to search for the optimal parameters which minimise the error in the least-squares sense defined by

$$E(\boldsymbol{\theta}) = \sum_{i=1}^n \|\mathbf{y}_0(i) - \mathbf{y}(i)\|^2, \quad (8)$$

where  $\mathbf{y}(i)$  is the  $i^{\text{th}}$  original output data sample;  $\mathbf{y}_0(i)$ , the estimated  $i^{\text{th}}$  output sample from the simulated model using parameters  $\boldsymbol{\theta}$  with the original input data;  $n$ , the number of data samples; and  $\|\cdot\|$ , the vector norm. The initial parameter values  $\boldsymbol{\theta}_0$  required in the Gauss-Newton method can be estimated by using subspace methods [18]. This estimation procedure was implemented by the PEM function of MATLAB.

The identification process is schematised in Figure 2. To identify the model given by (6), or more specifically, matrices  $\mathbf{A}$  and  $\mathbf{B}$ , at a given speed, the time history of the input steering torque  $\tau$  and the corresponding outputs composed of  $\delta$  and  $\theta$  must be generated. However, as the bicycle can be unstable at certain speeds, a roll-angle controller is necessary to produce sufficiently long simulations. The controller can be of any type, such as PID or fuzzy [15][16]; moreover, the accuracy of the control is not an important issue since the only requirement is to prevent falls during these simulations to ensure that sufficient input-output data are obtained. Nevertheless, as the input-output identification data are obtained from closed-loop simulations, the input signal (steering torque) may not be sufficiently persistently exciting. To reinforce the excitation of the identification data, random signals are generated and added to the input torque. The identified linear model can then be verified by comparing the output responses of the linear and nonlinear systems by feeding the same control torque into both systems.

### 3.2 Roll-angle tracking control by sliding-mode control

Sliding-mode control (SMC), as depicted in Figure 3, is a powerful approach to controlling nonlinear and uncertain systems. It is a robust control method which can be applied to the case with the presence of bounded model uncertainties and parameter disturbances. As Whipple's bicycle model is speed-varying, SMC can be applied to overcome the speed-dependant modelling errors. Consider the linear model in (6) and let  $\tilde{\theta} = \theta - \theta_{\text{ref}}$  be the roll-angle tracking error, where  $\theta_{\text{ref}}$  is the roll-angle reference.

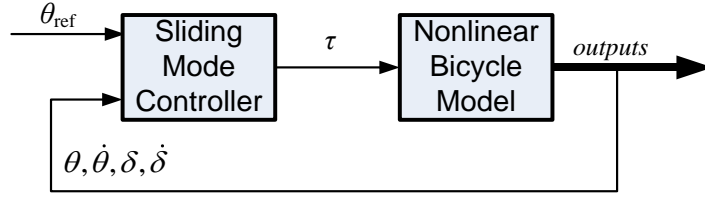


**Figure 3.** Sliding-mode controller (SMC) structure.

In this study, the sliding surface is defined as a plane of two states:  $\tilde{\theta}$ , the roll-angle tracking error, and  $\dot{\tilde{\theta}}$ , its derivative, corresponding to an exponentially stable first-order LTI system

$$s = \dot{\tilde{\theta}} + \lambda \tilde{\theta} = 0, \quad (9)$$

where  $\lambda$  is a strictly positive constant. A Lyapunov function  $V$  is defined as  $V = \frac{1}{2} s^2$ . The derived control law guarantees that  $V$  is always decreasing, or mathematically  $\dot{V} = s\dot{s} < 0$ . To verify this condition, the control  $\tau$  must be chosen so that  $\dot{s}$  and  $s$  have opposite signs. From the time derivative of (9), one can have

$$\dot{s} = \ddot{\tilde{\theta}} + \lambda \dot{\tilde{\theta}} = \ddot{\theta} - \ddot{\theta}_{ref} + \lambda \dot{\tilde{\theta}}. \quad (10)$$

Substituting  $\ddot{\theta}$  extracted from (6) into (10) gives

$$\dot{s} = (\mathbf{A}_2 \mathbf{x} + b_2 \tau) - \ddot{\theta}_{ref} + \lambda \dot{\tilde{\theta}}, \quad (11)$$

where  $\mathbf{A}_2$  is the second row of matrix  $\mathbf{A}$ , i.e.,  $\mathbf{A}_2 = [a_1 \ a_2 \ a_3 \ a_4]$ . By letting  $\dot{s} = 0$ , the equivalent control can be obtained as

$$\tau_{eq} = -\frac{1}{b_2} \left[ \mathbf{A}_2 \mathbf{x} - \ddot{\theta}_{ref} + \lambda \dot{\tilde{\theta}} \right]. \quad (12)$$

Consider the control law

$$\tau = \tau_{eq} - k \operatorname{sgn}(s), \quad (13)$$

where  $k$  is a controller gain. It can be proven that (13) satisfies the condition  $s\dot{s} < 0$  by substituting (12) into (13), which gives

$$\dot{s} = -b_2 k \operatorname{sgn}(s). \quad (14)$$

However, it can be remarked that (13) is not continuous when  $s$  switches from negative to positive or vice versa. When the system states are at the neighborhood of the sliding surface, this lack of continuity makes the system chattering. Therefore, the sign function is replaced by the saturation function to make the control law continuous when  $s$  is around zero, and the control law becomes

$$\tau = \tau_{eq} - k \operatorname{sat}(s / \Phi), \quad (15)$$

where  $\Phi > 0$  is the thickness of the boundary layer bordering the sliding surface which is introduced to avoid chattering; and  $\operatorname{sat}(s, \Phi)$ , the saturation function defined as

$$\operatorname{sat}(s, \Phi) = \begin{cases} 1, & s > \Phi, \\ s / \Phi, & -\Phi \leq s \leq \Phi, \\ -1, & s < -\Phi. \end{cases} \quad (16)$$

By appropriately choosing the control parameters  $\lambda$ ,  $k$  and  $\Phi$ , the bicycle can reach the roll-angle reference in a finite time and follow that reference without chattering. A detail discussion of the SMC used for roll-angle-tracking control can be found in [16].

### 3.3 Path-following control with preview

For path-tracking control in this study, the goal is to minimise the distance error  $e_L$  and the direction error  $e_\gamma$ , as shown in Figure 4. In real riding experience, the human rider usually looks forward at a preview point ahead on the direction that the motorcycle is moving. Normally, the distance of preview depends on the speed. If the speed is lower, the preview point would be nearer; if the speed is higher, the preview point would be farther accordingly. In this study, the preview distance is related to the speed by a simplified relation:

$$L_{\text{pre}} = v_x \times T_{\text{pre}} \quad (17)$$

where  $L_{\text{pre}}$  is the preview distance and  $T_{\text{pre}}$ , the preview time. The crosspoint of the lateral axis from the preview point and the target path is called target point. The preview distance error  $e_L$  is the distance from the preview point to the target point. When the target path is on the right side of the bicycle,  $e_L$  is positive and vice versa. The preview direction error  $e_\gamma$  is the angular difference between the motorcycle yaw angle and the direction of the target path at the preview point.

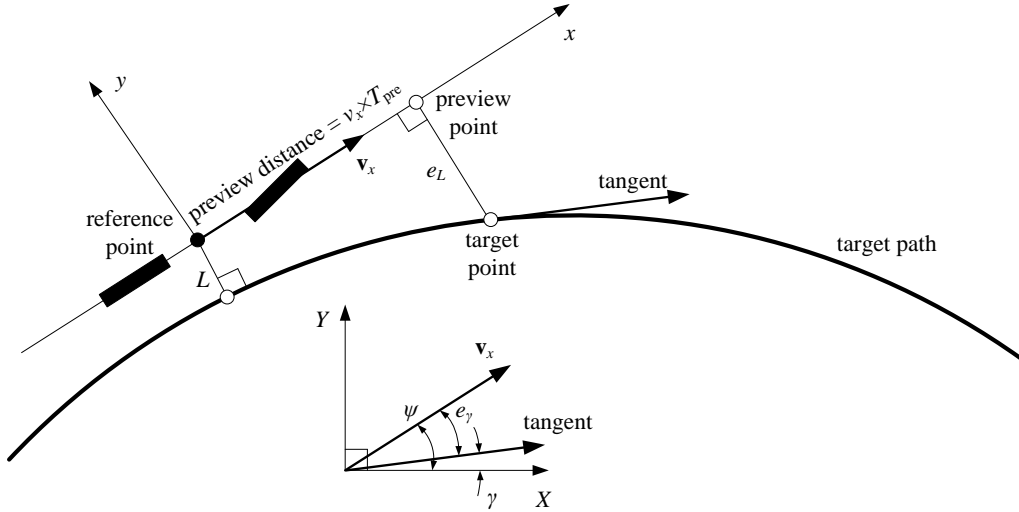


Figure 4. Error estimation for path-tracking control with path preview.

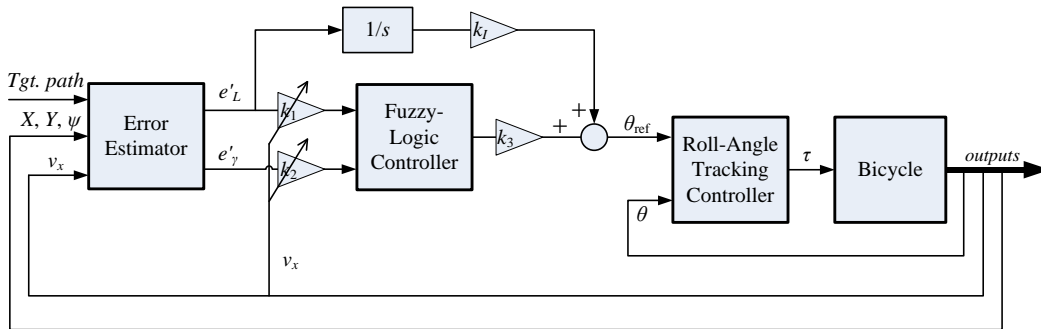


Figure 5. Path-tracking controller with disturbance rejection.

The path-tracking controller structure is presented in Figure 5. Unlike the path-tracking control of four-wheeled and three-wheeled vehicles, the control of single-track vehicles is more challenging. For a four-wheeled or three-wheeled vehicle, only the planar motion information, position and orientation, is needed to perform the path-tracking control, while for a single-track one such as a motorcycle, the roll stability must be additionally taken into consideration. In this study, the path-tracking control is proposed by generating an appropriate reference roll angle for

the roll-angle controller in the inner loop, which the stability problem is solved as presented in the previous subsection.

Another control loop is added to the existing roll-angle tracking controller. This control loop uses a fuzzy controller whose inputs are  $e_L$  and  $e_\gamma$ . From the planned path and the current position of the bicycle, the distance error  $e_L$  and the direction error  $e_\gamma$  are estimated. The two errors are passed through an FLC to generate target roll angle  $\theta_{ref}$ , which is then fed to the roll-angle-tracking controller discussed in the previous chapter. Linguistic quantification used to specify a set of rules for the new controller is characterized by the following typical situations:

(1) *If  $e_L$  is -6 and  $e_\gamma$  is -6, then  $\theta_{ref}$  is 0*

This rule quantifies the situation wherein the target path is on the left side of the bicycle and the angular difference is negative large. In this situation, we need not do anything since we want the bicycle to run quickly to the target path.

(2) *If  $e_L$  is 0 and  $e_\gamma$  is 0, then  $\theta_{ref}$  is 0*

This rule quantifies the situation wherein the bicycle is already in its proper position. No control effort is needed.

(3) *If  $e_L$  is 6 and  $e_\gamma$  is 6, then  $\theta_{ref}$  is 0*

In this case, one need not do anything for the same reason stated in the first situation.

(4) *If  $e_L$  is 6 and  $e_\gamma$  is -6, then  $\theta_{ref}$  is 6*

This rule quantifies the situation wherein the target path is on the right side of the bicycle and the bicycle is heading to the wrong side. Therefore, one needs to lean the bicycle to the right at a large angle.

In a similar fashion, the complete rule-base is constructed as listed in Table 1, where the membership functions -6, -5, -4, -3, -2, -1, 0, 1, 2, 3, 4, 5, 6 are used for the fuzzy variables, as shown in Figure 6. Notice that the body of the table lists the linguistic-numeric consequents of the rules, and the left column and top row of the table contain the linguistic-numeric premise terms. For this controller, with two inputs and seven linguistic values for each of these, there are totally  $13^2 = 169$  rules.

**Table 1.** Fuzzy rule base for path-tracking control with  $e_L$  and  $e_\gamma$  as inputs.

$e_\gamma \backslash e_L$	-6	-5	-4	-3	-2	-1	0	1	2	3	4	5	6
-6	0	1	2	2	3	3	4	4	5	5	6	6	6
-5	-1	0	1	2	2	3	3	4	4	5	5	6	6
-4	-2	-1	0	1	2	2	3	3	4	4	5	5	6
-3	-2	-2	-1	0	1	2	2	3	3	4	4	5	5
-2	-3	-2	-2	-1	0	1	2	2	3	3	4	4	5
-1	-3	-3	-2	-2	-1	0	1	2	2	3	3	4	4
0	-4	-3	-3	-2	-2	-1	0	1	2	2	3	3	4
1	-4	-4	-3	-3	-2	-2	-1	0	1	2	2	3	3
2	-5	-4	-4	-3	-3	-2	-2	-1	0	1	2	2	3
3	-5	-5	-4	-4	-3	-3	-2	-2	-1	0	1	2	2
4	-6	-5	-5	-4	-4	-3	-3	-2	-2	-1	0	1	2
5	-6	-6	-5	-5	-4	-4	-3	-3	-2	-2	-1	0	1
6	-6	-6	-6	-5	-5	-4	-4	-3	-3	-2	-2	-1	0

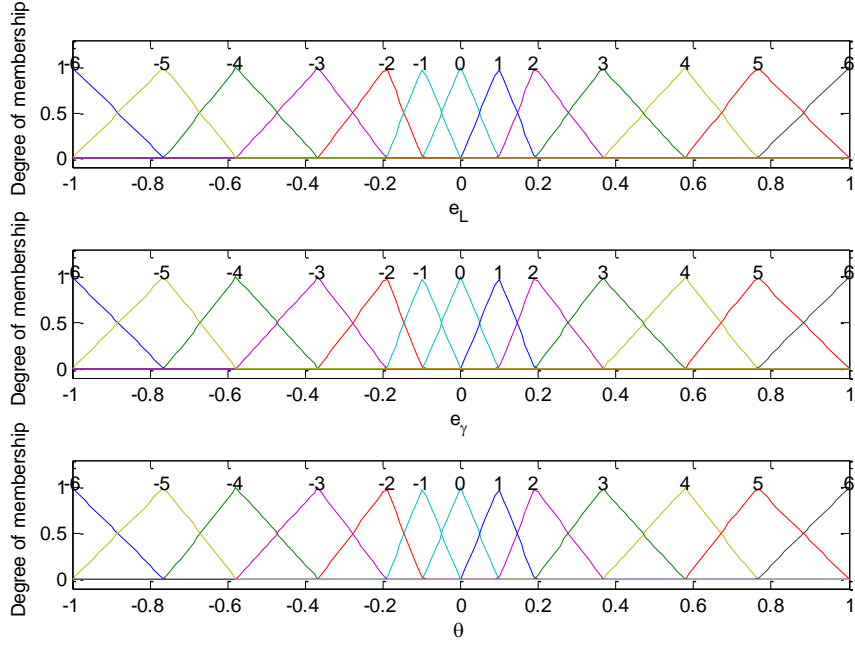


**Figure 6.** Fuzzy membership functions for path-tracking control.

To overcome the parameter variation due to the speed change of the bicycle, the gain-scheduling technique used in the study of Sharp et al. [12] for roll-angle control is reused, wherein the speed-dependent PID gains are replaced by speed-dependent scaling factors  $k_{1,2}$ . As the membership functions are normalized to  $[-1, 1]$ ,  $k_3$  represents the maximum absolute value of the generated reference roll angle, hence fixed to 60 degrees. In the study of Sharp et al., each of the PID gains depends on the vehicle speed by a polynomial relation. This introduces a set of subjacent parameters to the controller. The advantage of using PID is its simplicity; however, one of the difficulties in implementation of their controller is the choice of the speed-dependent parameters. Moreover, in this study, in order to attenuate the effect of external disturbances on the system, an integral term is added as the third term.

In this study, by profiting the property of the bicycle that it normally runs at a smaller range of speed in comparison with the motorcycle. The bicycle speed is supposed to be variable in the range from 5 to 30km/h; however, it could be extended without difficulty. This range is divided into many levels with the increment of 1km/h to tune the SFs. In order to make the controller be speed-adaptive, the DCs and SFs  $k_{1,2}$  are first tuned for a speed of 15km/h, then the membership functions are fixed and only the SFs are tuned for all the other speed levels from 5 to 30km/h, also by using genetic algorithms (GAs). After running the GAs, the optimal SFs are collected to establish two fitting polynomials which are functions of the bicycle speed.

For the path-tracking control, the goal is to minimize simultaneously the tracking error  $L$  and its oscillation. Therefore, the fitness function used for optimization is defined as

$$fitness\ value = \kappa_e^* \left( \frac{1}{N} \sum_{i=1}^N L^2(i) \right)^{1/2} + \kappa_{\Delta e}^* \left( \frac{1}{N} \sum_{i=1}^N \left( \frac{\Delta L(i)}{\Delta T} \right)^2 \right)^{1/2}, \quad (18)$$

where  $\Delta L(i) = L(i) - L(i-1)$  is the change in tracking error at time step  $i$ . The fitness function is the aggregation of two terms. The first is the root mean square of the tracking error multiplied by a weighting factor  $\kappa_e^*$ , and the second is the root mean square of the change in roll angle multiplied by a weighting factor  $\kappa_{\Delta e}^*$ .

#### 4 SIMULATION RESULTS

#### 4.1 Model identification

For the simulations in this study, the parameters are derived from the benchmark bicycle proposed in [5] and listed in Table 2. During the system identification process, the bicycle is controlled to follow a sinusoidal roll-angle with increasing frequency, by using a PD controller, the parameters of which are  $k_p = 88$  and  $k_D = 30$ . Uniformly-distributed pseudo-random number signals with an amplitude smaller than 1Nm are generated and added to the input steering torque to make the input signal persistently exciting. Figure 7 graphs the identification data from a simulation with an initial forward speed of 15km/s and a time step of 0.01s. This data is then entered in the PEM function of MATLAB to identify the continuous canonical state-space model. This procedure results in

$$\mathbf{A} = \begin{bmatrix} 0 & 1 & 0 & 0 \\ 5.342 & -0.406 & -12.349 & -3.149 \\ 0 & 0 & 0 & 1 \\ 13.042 & 21.024 & 22.374 & -16.840 \end{bmatrix}, \quad (19)$$

$$\mathbf{B} = \begin{bmatrix} 0 \\ -19.709 \\ 0 \\ 233.608 \end{bmatrix}, \text{ and } \mathbf{C} = \begin{bmatrix} 1 & 0 & 0 & 0 \\ 0 & 0 & 1 & 0 \end{bmatrix}.$$

**Table 2.** Simulation parameters derived from [5].

(a)

Name	Value	Name	Value
$m_a$	85 (kg)	$m_b$	2 (kg)
$m_d$	3 (kg)	$m_f$	4 (kg)
$\rho_a$	(0.5351, 0, 0.1275) (m)	$\rho_b$	(-0.3649, 0, 0.5275) (m)
$\rho_d$	(0.0321, 0, 0.5887) (m)	$\rho_e$	(0.4427, 0, -0.0725) (m)
$\rho_f$	(0.0261, 0, 0.2188) (m)	$\varepsilon$	18°
$r_f$	0.35 (m)	$r_r$	0.3 (m)
$g$	9.81 (m/s <sup>2</sup> )		

(b)

Component	Moment of inertia (kg.m <sup>2</sup> )
Vehicle body	$\mathbf{I}_A = \begin{bmatrix} 9.2 & 0 & 2.4 \\ & 11 & 0 \\ & & 2.8 \end{bmatrix}$
Front fork	$\mathbf{I}_F = \begin{bmatrix} 0.05892 & 0 & -0.00756 \\ & 0.06 & 0 \\ & & 0.00708 \end{bmatrix}$
Wheels	$\mathbf{I}_B = \begin{bmatrix} 0.0603 & 0 & 0 \\ & 0.12 & 0 \\ & & 0.0603 \end{bmatrix}, \mathbf{I}_D = \begin{bmatrix} 0.1405 & 0 & 0 \\ & 0.28 & 0 \\ & & 0.1405 \end{bmatrix}$

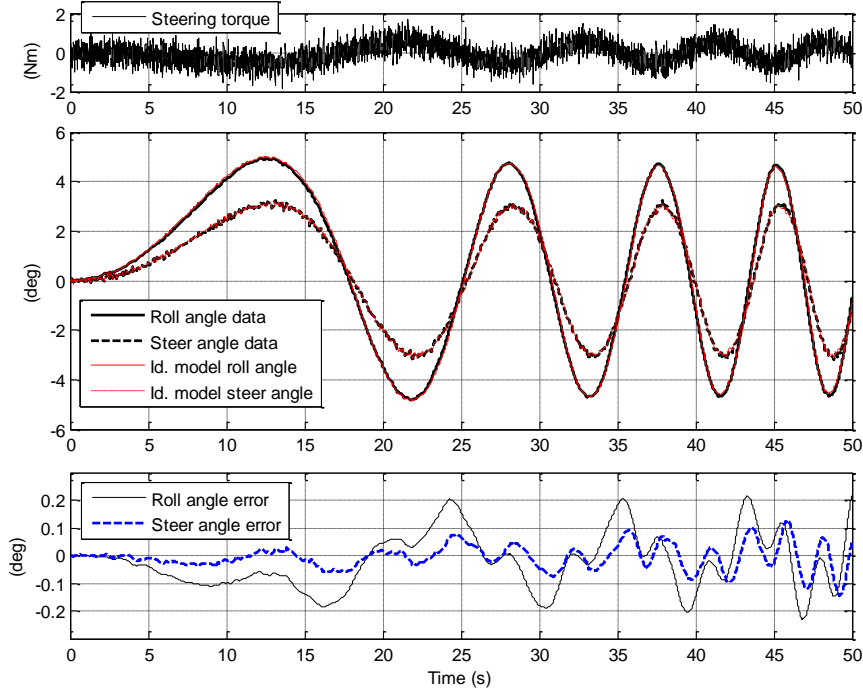


**Figure 7.** Identification data for simulation and verification at a speed of 15km/s.

The four poles calculated from  $\mathbf{A}$  are  $-15.041, -1.657$  and  $-0.274 \pm 3.344j$ . The obtained linear model is then used in an open-loop steering simulation by entering the original steering torque for verification. The results graphed in Figure 7 show that the output roll and steering angles follow the original data with only minor errors. Note that in this figure, the thin lines (identified model outputs) coincide within the thick ones (identification data) because of small model errors. The largest errors in the total 50s simulation time are  $0.230^\circ$  for the roll angle and  $0.145^\circ$  for the steering angle. This comparison verifies the fitting accuracy of the identified model.

#### 4.2 Roll-angle-tracking control

In this study, the bicycle is controlled to follow a sinusoidal reference roll angle with a time period of 4 seconds and an amplitude of  $10^\circ$ . The control simulation is implemented by using MATLAB/Simulink, wherein the nonlinear model is programmed in a C-language S-function. In the identified model in (19),

$$\mathbf{A}_2 = [5.342 \quad -0.406 \quad -12.349 \quad -3.149] \text{ and } b_2 = -19.709, \quad (20)$$

the control parameters of which are  $k = -100$ ,  $\lambda = 50$  and  $\Phi = 50$ . Figure 8 shows the control performance at a constant speed of 15km/h from the SMC controller and the corresponding steering torque. It appears that the controller can control the nonlinear model with small roll-angle tracking errors. After a transient time of nearly 0.2 seconds, the tracking error becomes stable with a maximal error of  $0.005^\circ$ . It can also be observed that the peak value of the steering torque generated by the SMC is 1.387Nm.

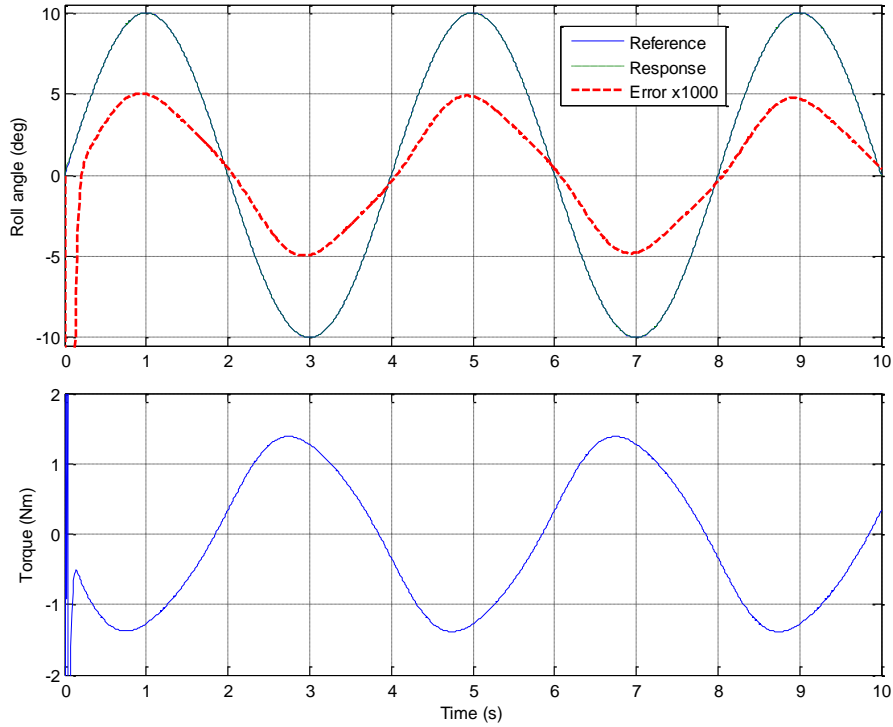


**Figure 8.** Roll-angle control performance at a speed of 15km/h.

Since the control parameters are designed on the basis of the model at a speed of 15km/h, the performance of the controller will degrade when the bicycle speed is changed. To evaluate the robustness due to speed change, the roll-angle tracking errors from the same control parameters are presented in Figure 9, depicting changes in speed to 5, 30 and 50km/h. It appears that for the SMC, with the parameters designed the model at the speed 15km/h, the maximal tracking error increases to only  $0.041^\circ$  for 30km/h,  $0.052^\circ$  for 50km/h and  $0.057^\circ$  for 5km/h, thus demonstrating that the designed SMC can control the bicycle in a wide range of speeds without a need for changing the control parameters. Note that because the linear bicycle model identified speed is 15km/h was used to design the SMC controller, the bicycle can be controlled more accurately at 15km/h than at other speeds. With a smaller tracking error, the controller generates a smaller torque. However, at higher or lower speeds, due to the model error, larger tracking errors are generated and thus, also larger control torque induced from the control law.

In Figure 10, the same roll-angle profile is used as a reference for control. However, a simple speed controller is used in the meantime to control the speed from 5 to 30km/h in 5 seconds and back to 5km/h, also in 5 seconds. It appears that with the PID, the tracking error of the SMC is kept at less than  $0.2^\circ$ , thereby demonstrating that the SMC is robust against speed variation.

In Figure 11, the bicycle is controlled at the original speed of 15km/h but in the presence of an external disturbance. This disturbance is injected as a lateral force from the left, applied to the bicycle body at reference point  $c$  in the direction of  $\mathbf{j}_c$ , at different magnitudes of 100, 200 and 300N from the 3<sup>rd</sup> to the 7<sup>th</sup> seconds. It can be observed that the behaviour of the bicycle is perturbed, whereby the tracking error increases proportionally to the magnitude of the disturbance. However, the disturbance has very small effects on the tracking error. For the disturbance of 300N, the tracking error is smaller than  $0.3^\circ$ . It can also be noticed that after the disturbance is released, the tracking error converges very quickly, after only 0.15 seconds.

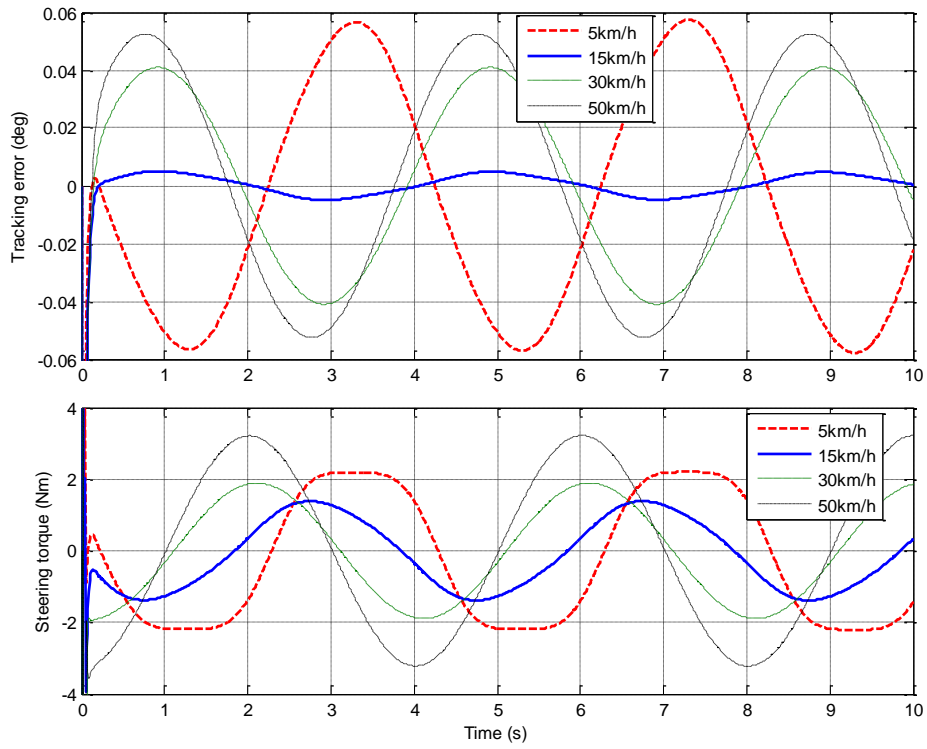


**Figure 9.** Control performance of SMC at different speeds.

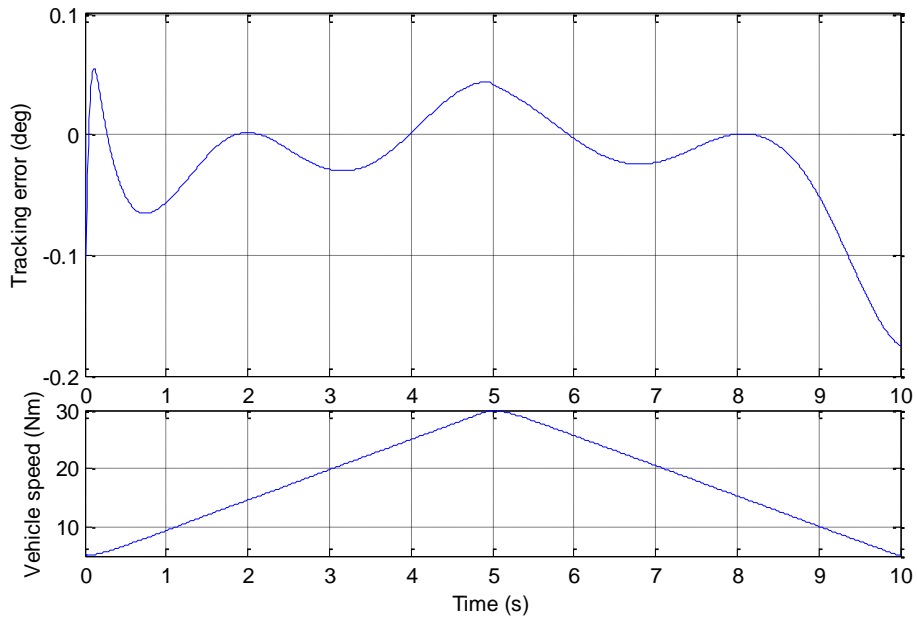


**Figure 10.** Control performance of SMC at varying speed.

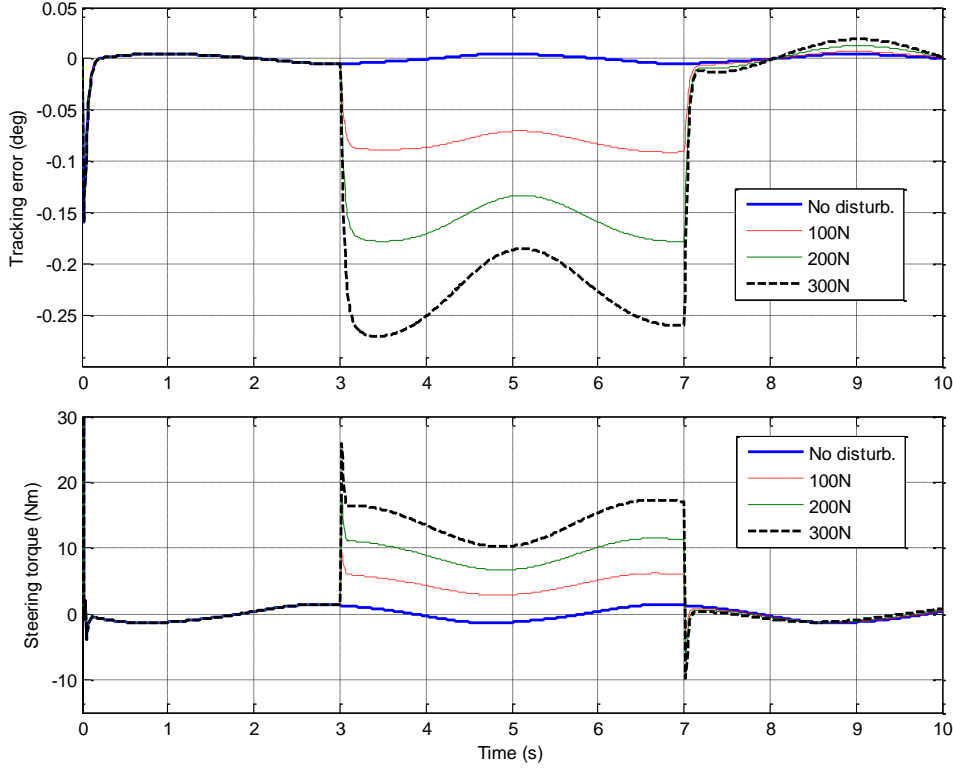


**Figure 11.** Control performance at a speed of 15km/h in presence of disturbance.

### 4.3 Path-tracking control

A simulation is carried out with the above controller, where the parameters are optimized using GAs at a speed 15km/h (see Figure 12), to control the bicycle model following a sinusoidal curve defined by the equation  $Y = 2.5\sin(2\pi X / 50)$  and the initial lateral position of the bicycle is 2m. The weighting factors for optimization are chosen as  $\kappa_e^* = 0.8$  and  $\kappa_{\Delta e}^* = 0.2$ . The optimized parameters are given in Table 3.

It is observed that, for lower speeds, smaller tracking error is achieved but the oscillation is more significant during the transient time, and vice versa for higher speeds. Therefore, the weighting factors are chosen as  $\kappa_e^* = 0.2$  and  $\kappa_{\Delta e}^* = 0.8$  for the speeds below 10km/h so that the oscillation has more importance on the fitness function; and as  $\kappa_e^* = 0.8$  and  $\kappa_{\Delta e}^* = 0.2$  for the speeds starting from 10km/h so that the tracking error has more importance on the fitness function. The fuzzy SFs for the path-tracking controller collected from running GAs are presented are shown in Figure 13. The obtained SFs are then used to establish the fitting curves with the following equations

$$\begin{aligned} k_{1B}(v_x) &= 2.01 \times 10^{-5} v_x^4 - 1.55 \times 10^{-3} v_x^3 + 0.04 v_x^2 - 0.34 v_x + 1.23, \\ k_{2B}(v_x) &= 9.77 \times 10^{-6} v_x^4 - 7.4 \times 10^{-4} v_x^3 + 0.021 v_x^2 - 0.28 v_x + 2.12, \end{aligned} \quad (21)$$

where  $v_x$  is valued in km/h. After establishing the fitting curves for  $k_1$  and  $k_2$ , simulations with varying speed was carried out. The speed is controlled by a simple PID controller to follow a reference command composed of two ramp-function pieces of the longitudinal position. First, the speed is controlled to increase from 5 at the initial position to 30km/h at a longitudinal position of 50m, then decrease back to 5km/h at the longitudinal position of 100m. In the meantime,

the bicycle was controlled to follow the same target path. As shown in Figure 14, the absolute value of the tracking error is kept under 0.08m in this simulation.

To investigate the effect of external disturbances on the bicycle, the bicycle model is controlled to follow the designed target path at a speed of 10km/h, but in the presence of an external disturbance, and the control performance presented in Figure 15. This disturbance is injected as a lateral force of 200N from the left, applied to the bicycle body at reference point  $c$  in the direction of  $\mathbf{j}_c$ , in a range of longitudinal position from 20m to 60m. It can be observed that during the presence of the disturbance, the system dynamics perturbed and the tracking error is shifted to the same direction of the disturbance with a steady-state value of nearly 0.8m. After the disturbance is released, the behaviour of the bicycle is restored quickly with the help of the path-tracking controller.

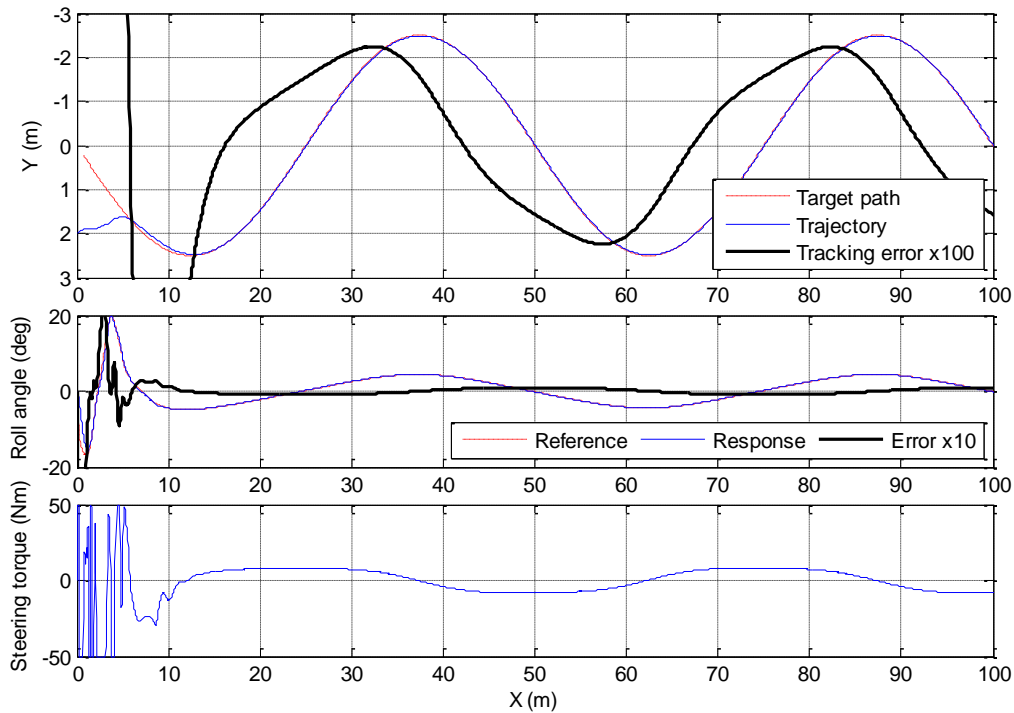


**Figure 12.** Path-tracking control at a speed of 15km/h and a preview time of 0.5 seconds.

**Table 3.** Optimized parameters for the path-tracking controller at a speed of 15km/h.

Fuzzy variable	DC	SF
Input $e_L$	0.476	0.984
Input $\Delta e_L$	0.653	0.367
Output $\theta_{ref}$	0.391	60
<b>Fitness value</b>	<b>0.0261</b>	

This phenomenon can be explained as follows. When the disturbance appears, the roll-angle-tracking controller tries to balance the bicycle. Since the disturbance has direction from left to right, the bicycle is leaned more to the left so that the gravity can balance with the disturbance (unlike in a roll-angle-tracking control where the bicycle trajectory is not of interest and the balance is fulfilled with help of the centrifugal force caused by a steering angle). This can be observed from Figure 15 by the fact that the roll angle is reduced by about 8 degrees during the

presence of the disturbance. When the disturbance is released, the equilibrium point is also re-stored.

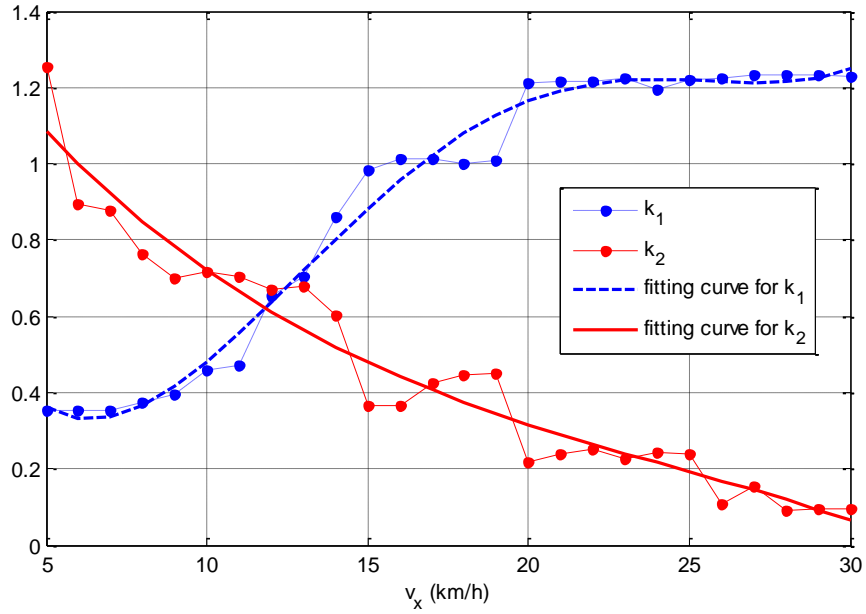


**Figure 13.** Speed-dependent fuzzy SFs and fitness values for path-tracking control.

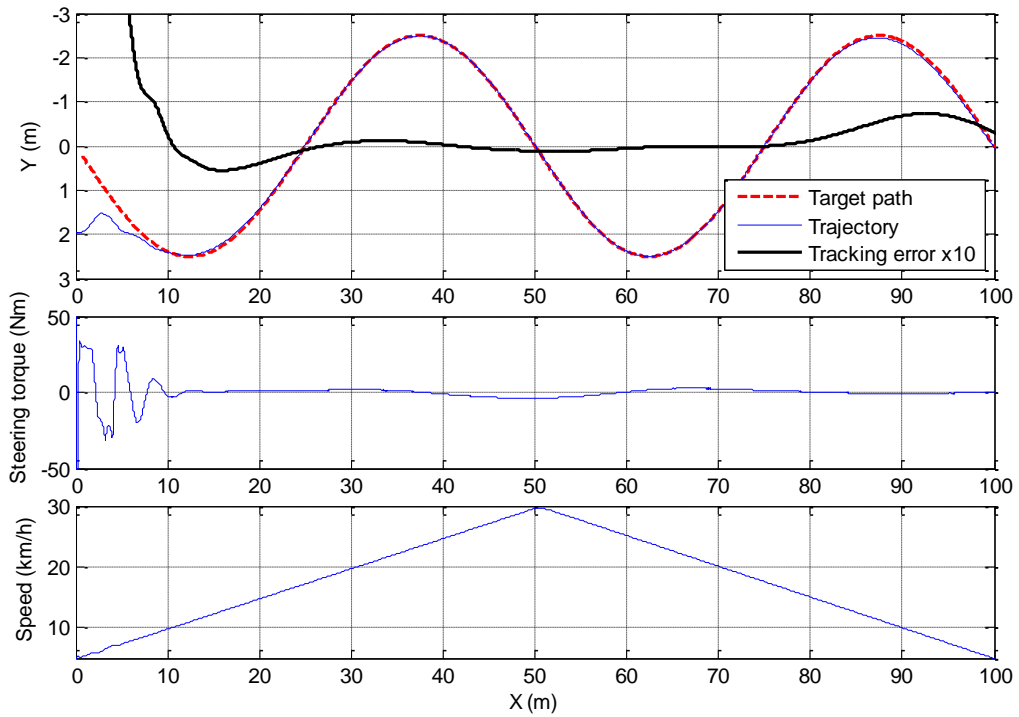


**Figure 14.** Path-tracking control at varying speed.

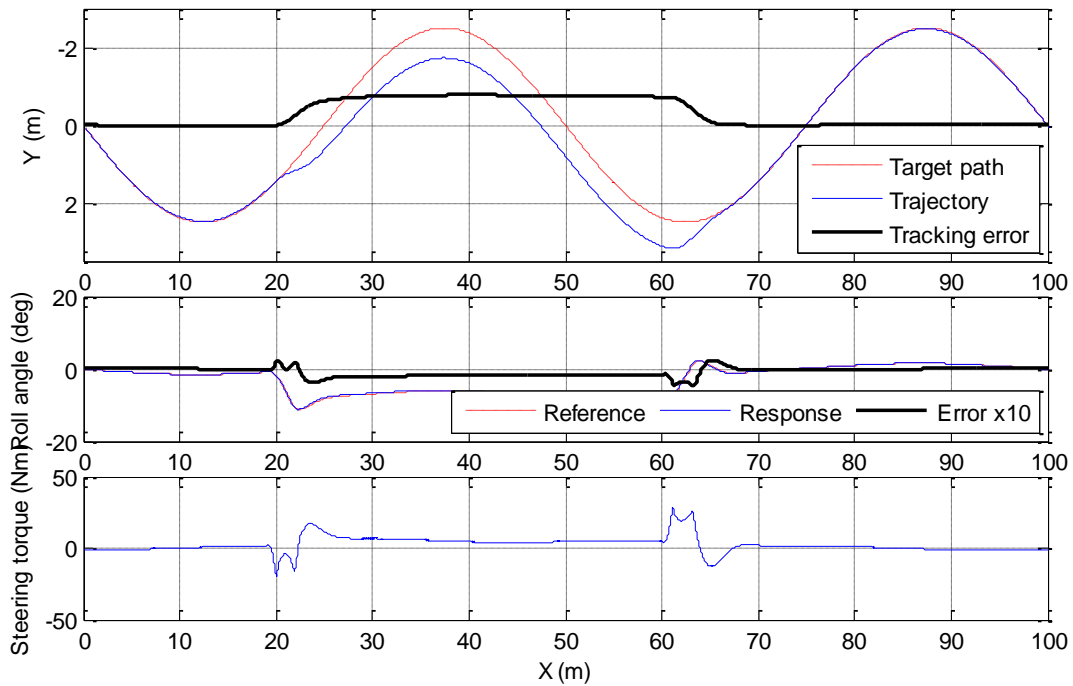


**Figure 15.** Path-tracking control in presence of disturbance at a speed of 10km/h.

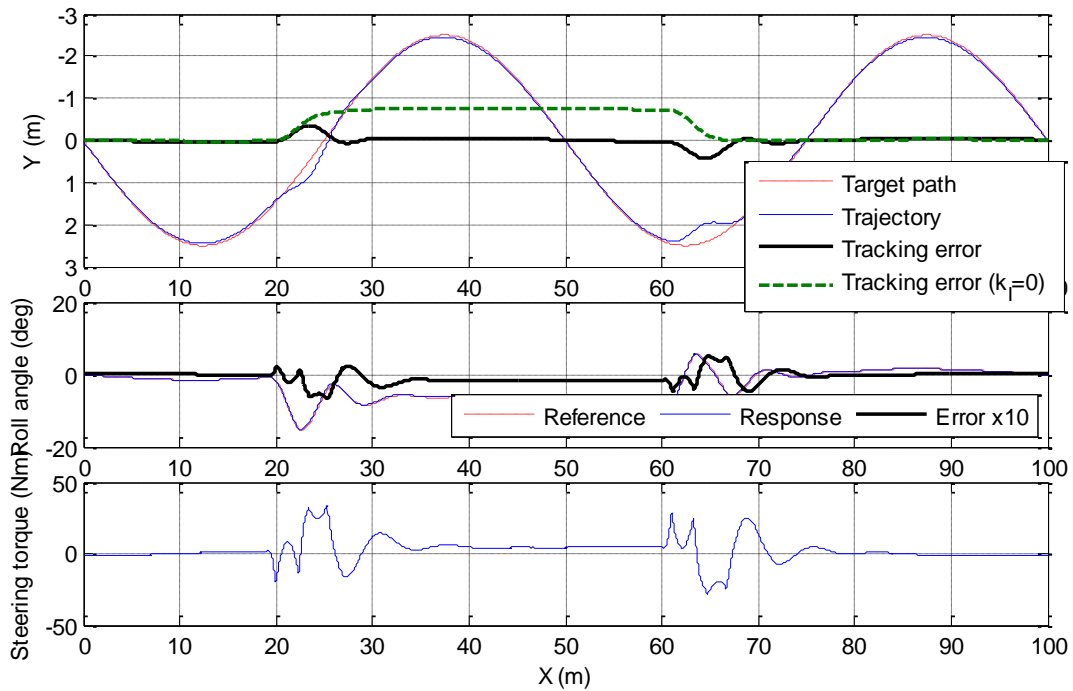


**Figure 16.** Path-tracking control with disturbance rejection at a speed of 10km/h.

This problem can be solved by adding an integrator and an adjustable gain  $k_I$  between the preview distance error  $e_L$  and the reference roll angle. Simulations with this controller (also at a speed of 10km/h) are shown in Figure 16, where the value of  $k_I$  is 15. As soon as the disturbance is applied, the tracking error increases. However, by the effect of the integrator, an additional term is added to the reference roll angle, helping the bicycle to be pulled back to the direction making the tracking error reduced. When the disturbance is released and the equilibrium

point changes, a similar process also happens, however, in the inverse direction. The overshoot is about 0.3m, and the transient longitudinal distance is about 7m. The control gain  $k_f$  can be used to adjust the balance between the overshoot and the transient time.

## 5 CONCLUSIONS

In this study, system identification has been applied to identify the linear model from a developed nonlinear bicycle model at a speed of 15km/h. Subsequently, SMC was used to design a roll-angle-tracking controller based on the identified linear model. The robustness of the controller was evaluated by control simulations with different schemes. Without changing the control parameters designed for a specific speed, the bicycle can be controlled to follow the roll-angle reference with only a small tracking error at different constant speeds as well as at widely varying speeds. The robustness of the control was also evaluated in the presence of external disturbances. With external lateral forces applied to the bicycle body during the control time, the tracking error increased slightly and vanishes very quickly once the external forces are released. On the basis of the roll-angle-tracking controller, another control loop is added to address the path-tracking problem by using FLC with an integral controller. Simulations with a developed bicycle model show advantages of the proposed controller.

## ACKNOWLEDGEMENTS

The authors would like to thank the National Science Council of the Republic of China, Taiwan, for financially supporting this research under project number NSC 96-2221-E-212-027.

## REFERENCES

- [1] D. E. H. Jones, "The stability of the bicycle", *Physics Today*, 23 (1970), pp. 34-40.
- [2] H. Bouasse, *Cours de Mécanique Relationnelle et Expérimentale, part 2*, Library Ch. De-lagrange, Paris, 1910, pp. 620-623.
- [3] S. Timoshenko, and D. H. Young, *Advanced Dynamics*, McGraw-Hill, New York, 1948, pp. 239-240.
- [4] A. L. Schwab, J. P. Meijaard, and J. M. Papadopoulos, "Benchmark results on the linearized equations of motion of an uncontrolled bicycle", *KSME Int. J. of Mechanical Science and Technology*, **19** (2005), pp. 292-304.
- [5] J. P. Meijaard, J. M. Papadopoulos, A. Ruina, and A. L. Schwab, "Linearized dynamics equations for the balance and steer of a bicycle: A benchmark and review", *Proc. of the Royal Society, Series A*, **463** (2007), pp. 1955-1982.
- [6] J. P. Meijaard, and A. L. Schwab, "Linearized equations for an extended bicycle model", *Proc. of III European Conf. on Computational Mechanics, Solids, Structures and Coupled Problems in Engineering*, (2006), Lisbon, Portugal.
- [7] R. S. Sharp, "On the stability and control of the bicycle", *Applied Mechanics Reviews*, **61** (2008), 060803.
- [8] Y. Yavin, "Stabilization and control of the motion of an autonomous bicycle by using a rotor for the tilting moment", *Computer Methods in Applied Mechanics and Engineering*, **178** (1999), pp. 233-243.
- [9] A. V. Beznos, A. M. Formal'sky, E. V. Gurfinkel, D. N. Jicharev, A. V. Lensky, K. V. Savitsky, and L. S. Tchesalin, "Control of autonomous motion of two-wheel bicycle with gyroscopic stabilisation", *Proc. of IEEE Int. Conf. on Robotics and Automation*, **3** (1988), Leuven, Belgium, pp. 2670-2675.
- [10] S. Han, J. Han, and W. Ham, "Control algorithm for stabilization of tilt angle of unmanned electric bicycle", *Trans. on Control, Automation and Systems Engineering*, **3** (2001), pp.

176-180.

- [11] N. H. Getz, "Internal equilibrium control of a bicycle", *Proc. of IEEE Conf. on Decision and Control*, **4** (1995), New Orleans, USA, pp. 4285-4287.
- [12] R. S. Sharp, S. Evangelou, and D. J. N. Limebeer, "Advances in the modelling of motorcycle dynamics", *Multibody System Dynamics*, **12** (2004), pp. 251-283.
- [13] R. S. Sharp, "Motorcycle steering control by road preview", *J. of Dynamic Systems, Measurement, and Control*, **129** (2007), pp. 373-381.
- [14] C. K. Chen, and T. S. Dao, "Fuzzy control for equilibrium and roll-angle tracking of an unmanned bicycle", *Multibody System Dynamics*, **15** (2006), pp. 325-350.
- [15] C. K. Chen, and T. S. Dao, "Genetic fuzzy control for path-tracking of an autonomous robotic bicycle", *J. of System Design and Dynamics*, **1** (2007), pp. 536-547.
- [16] C. K. Chen, and T. K. Dao, "Speed-adaptive roll-angle-tracking control of an unmanned bicycle using fuzzy logic", *Vehicle System Dynamics*, **48** (2010), pp. 133-147.
- [17] F. J. W. Whipple, "The stability of the motion of a bicycle", *Q. J. of Pure and Applied Mathematics*, **30** (1899), pp. 312-348.
- [18] L. Ljung, *System Identification: Theory for the User*, Prentice-Hall, Inc., Upper Saddle River, New Jersey, 1999.